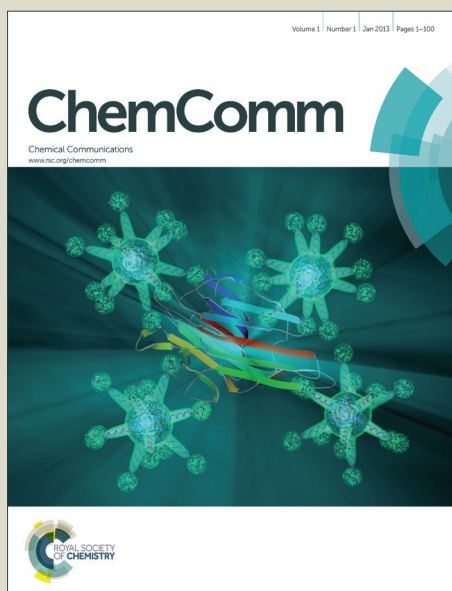


ChemComm

Accepted Manuscript



This article can be cited before page numbers have been issued, to do this please use: L. H. Zhi, H. Zhang, Z. Yang, W. Liu and B. Wang, *Chem. Commun.*, 2016, DOI: 10.1039/C6CC00780E.



This is an *Accepted Manuscript*, which has been through the Royal Society of Chemistry peer review process and has been accepted for publication.

Accepted Manuscripts are published online shortly after acceptance, before technical editing, formatting and proof reading. Using this free service, authors can make their results available to the community, in citable form, before we publish the edited article. We will replace this *Accepted Manuscript* with the edited and formatted *Advance Article* as soon as it is available.

You can find more information about *Accepted Manuscripts* in the [Information for Authors](#).

Please note that technical editing may introduce minor changes to the text and/or graphics, which may alter content. The journal's standard [Terms & Conditions](#) and the [Ethical guidelines](#) still apply. In no event shall the Royal Society of Chemistry be held responsible for any errors or omissions in this *Accepted Manuscript* or any consequences arising from the use of any information it contains.

Cite this: DOI: 10.1039/c0xx00000x

www.rsc.org/xxxxxx

ARTICLE TYPE

Interface Coassembly Mesoporous MoS₂ Based- Frameworks for Enhanced Near-Infrared Light Driven Photocatalysis

Lihua Zhi,^a Haoli Zhang,^a Zhenyin Yang,^a Weisheng Liu,^a and Baodui Wang*^a

Received (in XXX, XXX) Xth XXXXXXXXX 20XX, Accepted Xth XXXXXXXXX 20XX DOI: 10.1039/b000000x

Three-dimensional porous Fe₃O₄@Cu_{2-x}S-MoS₂ framework is firstly reported. The as-prepared 3D framework exhibits good structural stability, a high surface area, the enhanced adsorption capacity to substrates, and the strong absorption at NIR-range. As a result, such hybrid frameworks exhibit excellent NIR-light photocatalytic activity and stable cycling for the direct arylation of heteroaromatics at room temperature.

The ongoing global demand for energy has stimulated intense research on solar energy utilization,¹ because sunlight has been recognized as an environmentally friendly and sustainable form of energy. Especially, the near-infrared (NIR, 760–3000 nm) range of the solar spectrum accounts for 54.3% of the total energy as opposed to only 6.8% from the ultraviolet (UV) light.² Up to now, a large number of NIR responsive photocatalytic materials have been developed.³ However, the insufficient stability and low efficiency still render the overall process impractical. Thus, the design and exploitation of semiconductor-based heteronanostructures with NIR absorption, high efficiency, acceptable stability, and low cost are still critical and urgent task for efficient solar photosynthesis.

As a semiconducting two-dimensional (2D) “van der Waals” material, MoS₂ nanosheets (NSs) have attracted special attention in the materials science and engineering field due to its outstanding electronic,⁴ optical,⁵ and catalytic⁶ properties. Of particular interest, MoS₂ has been known as a photocatalyst and solar cell material due to its narrow indirect band gap of ~1.2 eV, which gives rise not only to its visible-light-harvesting function but also to its high stability against photocorrosion.⁷ For photocatalytic⁸ applications, it has been highly required to develop a new route to porous MoS₂ with high specific surface area. Especially when utilized as a catalyst in photocatalysis, the porosity may exert a significant effect on the accessibility of the target molecules to catalytically active sites. Exfoliation of MoS₂ into mono- or few-layers is a critical step toward making it optically active and implementing into novel devices. It should be pointed out that, due to the high surface energy and interlayer van der Waals attraction, aggregation and stacking commonly occur between individual randomly oriented NSs, which results in the loss of active sites or other unusual properties of ultrathin 2D nanostructures.⁹ To solve this problem, some strategies have been devoted to reassemble cluster particles or metal complexes with MoS₂ to form microporous pillared MoS₂ compounds.¹⁰ However, all the efforts so far seem to have been unsuccessful in enhancing the specific surface area and

the stability due to the structural instability of the between 2D MoS₂ NSs, since the linkage that holds the three-dimensional (3D) MoS₂ network together is physical in nature (e.g., van der Waals force and π - π conjugation). In addition, controllable assemble of chalcogenide nanomaterials into MoS₂ interlayer to form heterostructured MoS₂ based-frameworks has rarely been reported, especially for enhanced NIR- light-driven photocatalytic activity. We demonstrated that such heterostructured composites can endow the composites novel characteristics and some enhanced properties by the synergistic effect.

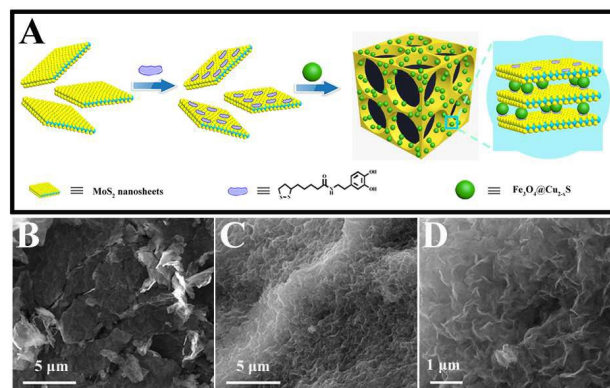


Figure 1. (A) Illustration of the preparation of 3D porous Fe₃O₄@Cu_{2-x}S-MoS₂F. SEM images of N-(3,4-dihydroxyphenethyl)-5-(1,2-dithiolan-3-yl) pentanamide-MoS₂ (DPA-MoS₂) (B) and 3D Fe₃O₄@Cu_{2-x}S-MoS₂F (C-D).

Herein, we present a facile strategy for the synthesis of 3D porous Fe₃O₄@Cu_{2-x}S-MoS₂ framework (F) via *in situ* covalent functionalization of MoS₂ with catechol substitutes followed by coordination with Fe₃O₄@Cu_{2-x}S nanoparticles (NPs). The obtained MoS₂ based- framework consists of units of MoS₂ NSs bridged by Fe₃O₄@Cu_{2-x}S nanoparticle linkages. Fe₃O₄@Cu_{2-x}S NPs were selected as the building blocks owing to their excellent tunable plasmonic absorption especially in the NIR region and superparamagnetic properties.¹¹ Thus, such NPs are promising candidates for building plasmon enhanced photocatalysts. Meanwhile, Fe₃O₄@Cu_{2-x}S NPs are homogeneously anchored into the skeleton of honeycomb-like MoS₂ nanoframeworks through coordination bond, which can effectively inhibit the aggregation of exfoliated MoS₂ NSs, and thus enhance the stability of active materials. In addition, the obtained honeycomb-like MoS₂ nanoframeworks could facilitate the transportation of reactants and products through the interior space due to the interconnected porous network. With these

merits, the resulting 3D $\text{Fe}_3\text{O}_4@\text{Cu}_{2-x}\text{S}-\text{MoS}_2\text{F}$ exhibited enhanced NIR light photocatalytic activity and stable cycling for the direct arylation of heteroaromatics at room temperature.

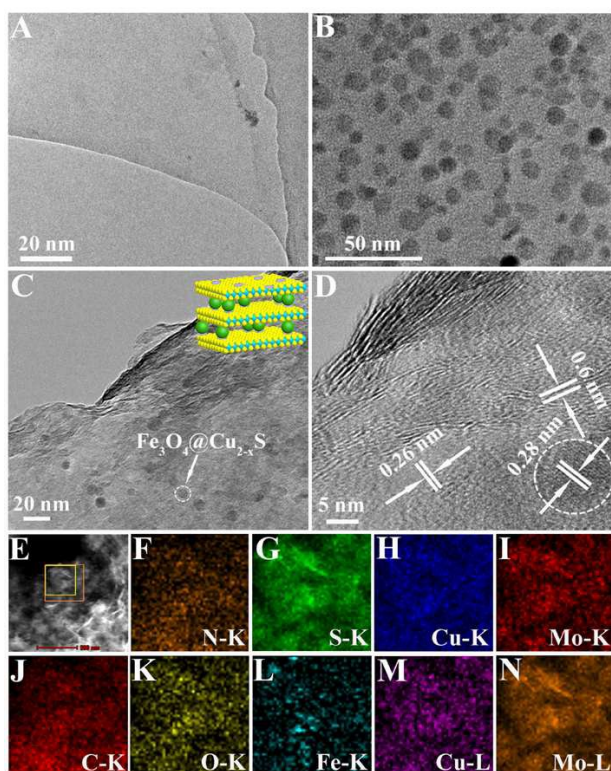


Figure 2. TEM images of DPA-MoS₂ (A), Fe₃O₄@Cu_{2-x}S (B) and 3D Fe₃O₄@Cu_{2-x}S-MoS₂F (C). (D) HRTEM image of 3D Fe₃O₄@Cu_{2-x}S-MoS₂F. (E) Dark field of STEM images. (F-N) Element mapping images of the 3D Fe₃O₄@Cu_{2-x}S-MoS₂F. The inset shows the simulation diagram of the formed 3D Fe₃O₄@Cu_{2-x}S-MoS₂F.

The overall scheme for the fabrication of 3D Fe₃O₄@Cu_{2-x}S-MoS₂F was illustrated in Figure 1A. Details of the process are given in the Methods section. Fe₃O₄@Cu_{2-x}S core-shell NPs were prepared in oleylamine by a modified literature method¹¹. A colloidal suspension of highly monodisperse monolayer MoS₂ sheets were exfoliated via lithium intercalation method followed by reaction with excess water. Subsequently, N-(3,4-dihydroxyphenethyl)-5-(1,2-dithiolan-3-yl) pentanamide (LA-DPA) was used to modify 2D MoS₂ NSs, in which the defect sites of MoS₂ NSs were anchored by sulfur atoms of LA-DPA to form DPA-MoS₂. The formed DPA-MoS₂ NSs were mixed with the as-synthesized Fe₃O₄@Cu_{2-x}S NPs by magnetic stirring for 24 hours, in which the catechol group modified on the MoS₂ NSs coordinated with the Cu⁺ ion existing on the surface of Fe₃O₄@Cu_{2-x}S to form 3D Fe₃O₄@Cu_{2-x}S-MoS₂F. Meanwhile, Fe₃O₄@Cu_{2-x}S NPs were densely anchored and embedded in the MoS₂ networks. It is important to note that this method can be readily extended to the synthesis of other types of metal oxide NP-MoS₂Fs, such as Fe₃O₄-MoS₂F and CuFe₂O₄-MoS₂F (Figures S1 and S2).

The morphology of the formed 3D Fe₃O₄@Cu_{2-x}S-MoS₂F was primarily investigated by scanning electron microscopy (SEM). From the Figure 1C and D, it can be clearly shown that the product has interconnected submicrometer-sized macroporous networks. The walls of the interconnected 3D porous networks demonstrate a clear curved profile and a very

low contrast, which were not found in 2D MoS₂ NSs (Figure 1B). These pores were formed by the cross-link coordination between MoS₂ NSs and Fe₃O₄@Cu_{2-x}S NPs. The microstructures of the 3D Fe₃O₄@Cu_{2-x}S-MoS₂F were further studied by transmission electron microscopy (TEM) and high-resolution TEM (HRTEM). Figure 2A shows that DPA-MoS₂ gives transparent sheets with folded boundaries. After the Fe₃O₄@Cu_{2-x}S NPs coordinated with DPA-MoS₂ to form 3D Fe₃O₄@Cu_{2-x}S-MoS₂F, Fe₃O₄@Cu_{2-x}S NPs were densely anchored and embedded between two sheets of MoS₂, and no large particles aggregates were observed in TEM images (Figure 2C). The HRTEM image (Figure 2D) reveals that a very thick layer like an sandwich structure was appeared in Fe₃O₄@Cu_{2-x}S-MoS₂F. The corresponding elemental mapping (Figure 2E-N) and energy dispersive X-ray (EDX) analysis (Figure S3) clearly verify the existence of C, N, O, S, Mo, Cu, and Fe elements with homogeneous distribution in Fe₃O₄@Cu_{2-x}S-MoS₂F. Moreover, the loading amount of Fe₃O₄@Cu_{2-x}S in the Fe₃O₄@Cu_{2-x}S-MoS₂F, based on the inductively coupled plasma spectroscopy (ICP-AES) test, is ~4.5 wt%. From the XRD pattern of the as-prepared 3D Fe₃O₄@Cu_{2-x}S-MoS₂F (Figure 3A), the three distinct sets of diffraction peaks are readily indexed to a mixture of the face-centered cubic Fe₃O₄ (JCPDS file number 65-3107), hexagonal Cu₉S₈ phases (JCPDS file number 36-0379)¹¹ and MoS₂ phase¹², respectively. Compared to the pure MoS₂ NSs, the lower angle shift of the (002) diffraction in the 3D Fe₃O₄@Cu_{2-x}S-MoS₂F is due to an enlarged interlayer spacing and the formation of a new lamellar structure.¹³ The Raman spectroscopy of 3D Fe₃O₄@Cu_{2-x}S-MoS₂F revealed the characteristic peaks of MoS₂ including E_{2g} at 378.7 cm⁻¹ and A_{1g} at 403.0 cm⁻¹ (Figure S4),¹⁴ suggesting that the crystalline MoS₂ exists in the nanohybrid framework.

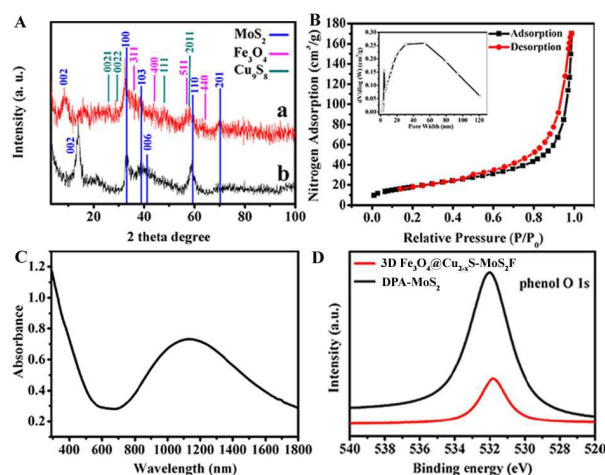


Figure 3. (A) XRD pattern of the 3D Fe₃O₄@Cu_{2-x}S-MoS₂F (a) and MoS₂ NSs (b). (B) Nitrogen adsorption-desorption isotherms of the 3D Fe₃O₄@Cu_{2-x}S-MoS₂F. Inset: the pore size distribution of the 3D Fe₃O₄@Cu_{2-x}S-MoS₂F. (C) Corresponding UV-vis-NIR absorption spectra of the 3D Fe₃O₄@Cu_{2-x}S-MoS₂F dispersed in DMF. (D) High-resolution scans for the phenol O 1s electrons.

Figure 3B shows nitrogen adsorption-desorption isotherms and the corresponding pore size distribution curves of 3D Fe₃O₄@Cu_{2-x}S-MoS₂F. The adsorption-desorption isotherms hybrids are of type IV, indicating the presence of mesopores (2-50 nm). In addition, the hysteresis loops which resemble the H2 type signifies irreversible desorption, suggesting the formation of relatively large mesopores and

macropores.¹⁵ The 3D Fe₃O₄@Cu_{2-x}S-MoS₂F exhibits a large portion of pores in the range of 5.2~120 nm (Figure 3B), which originate from the pore formation between the MoS₂ flakes after inserting Fe₃O₄@Cu_{2-x}S NPs, and a small portion of pores in the range of 3.7~5.2 nm is associated with the small meso- and micropores formed between MoS₂ sheets during their irreversible restacking, indicating that Fe₃O₄@Cu_{2-x}S NPs do not insert into sheets of a small amount of MoS₂.¹⁶ So, the two types of pore size distribution should be clearly attributed to different spatial structure of frameworks. Brunauer Emmett Teller (BET) analysis demonstrates a specific surface area of 66.85 m² g⁻¹ for the 3D Fe₃O₄@Cu_{2-x}S-MoS₂F, which is 340 times as much as MoS₂ nanosheets (0.19 m² g⁻¹).

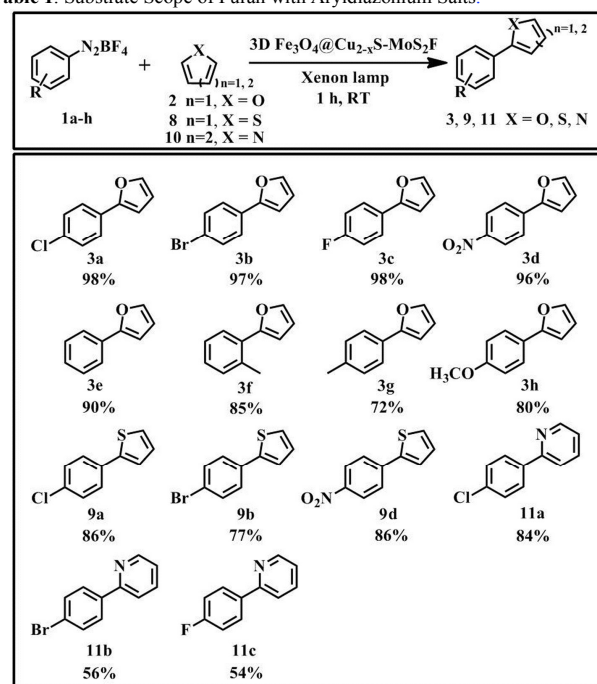
The UV-vis absorption spectroscopy of 3D Fe₃O₄@Cu_{2-x}S-MoS₂F solutions showed an intense broad band in the range of 700-1800 nm (Figure 3C), which is similar with the Fe₃O₄@Cu_{2-x}S NPs (Figure S8) due to the localized surface plasmon resonances in vacancy-doped semiconductors.¹⁷ In contrast, 2D MoS₂ nanosheets solutions did not exhibit any appreciable absorption in that spectral range (Figure S9). The above results indicated that the 3D Fe₃O₄@Cu_{2-x}S-MoS₂F was formed. In addition, the strong absorption in the NIR range implicates the potential application of this nano hybrids in NIR light photocatalysis. Furthermore, the formation of Fe₃O₄@Cu_{2-x}S-MoS₂F and their superparamagnetic property were confirmed by FT-IR spectra and vibrating sample magnetometer (VSM) (Figure S10 and S11 as well as related discussions in the supporting information). Moreover, a typical survey XPS spectrum in Figure S12A clearly shows the presence of copper, sulfur, carbon, oxygen, nitrogen, iron, and molybdenum in 3D Fe₃O₄@Cu_{2-x}S-MoS₂F. The high-resolution N1s and O1s spectrum shows the presence of amide (394.6 eV) and phenolic oxygen (531.7 eV), respectively (Figure S12). As shown in Figure 3D, the upshift of the phenolic O1s from 531.7 for Fe₃O₄@Cu_{2-x}S-MoS₂F to 532.0 eV for DPA-MoS₂ is attributed to the coordination of oxygen atoms to copper.¹⁸ Figure S12E shows the binding energies of Cu 2p3/2 and Cu 2p1/2 peaks at 932.2 and 952.3 eV, respectively, which can be attributed to the Cu⁺¹ state.¹⁹

Arylated heteroarenes are widely used in materials science due to their interesting optical and electronic properties²⁰ as well as biomedical applications as peptide mimetics²¹ or drugs.²² Recently, direct utilization of visible sunlight in combination with metal and metal-free catalysts²³ received significant attention as a promising method for the C-H arylation with diazonium salts.²⁴ Based on the strong absorption band of 3D Fe₃O₄@Cu_{2-x}S-MoS₂F in the range of 700–1800 nm, we decided to investigate the direct arylation of heteroarenes between diazonium salts with heteroarenes by using this heterogeneous catalyst and irradiating with NIR light (≥700 nm) at 25 °C for 1 h. Among the different solvents tested (Table S1), ethanol was found to be a good solvent for the photoreaction (Table S1 entry 6). Meanwhile, the photocatalytic activities of MoS₂, Fe₃O₄@Cu_{2-x}S, simply mixed Fe₃O₄@Cu_{2-x}S and MoS₂, and Fe₃O₄@Cu_{2-x}S-MoS₂F without light were also carried out. As shown in Figure S13, the use of Fe₃O₄@Cu_{2-x}S-MoS₂F catalyst resulted in > 98% yield under NIR light. However, no traceable products were detected for control experiments. Also, we found that the photocatalytic activity of the Fe₃O₄@Cu_{2-x}S sample and simply mixed Fe₃O₄@Cu_{2-x}S and MoS₂ was significantly

lower than that of the Fe₃O₄@Cu_{2-x}S-MoS₂F sample, which reveals that the 3D porous assembly structure plays an important role for the enhancement of the photocatalytic activity.

Subsequently, we investigated the substrate scope of the Fe₃O₄@Cu_{2-x}S-MoS₂F catalyst mediated direct C-H arylation (Table 1). Gratifyingly, substrates bearing both electron-withdrawing as well as donating and neutral functional groups could be activated. Thus, the corresponding products were obtained in yields up to 72% (3a-3h). Moreover, the Fe₃O₄@Cu_{2-x}S-MoS₂F photocatalyzed C-H arylation was also effective for other heteroarenes, such as thiophene and pyridine, and the corresponding products were obtained in moderate to good yields (9a-11c). Interestingly, our catalyst could achieve moderate to good yields in very short time (within 1h), which is better than that of other reported photocatalysts.²⁵

Table 1. Substrate Scope of Furan with Aryldiazonium Salts.



Reaction conditions: 0.1 mmol 1a-h, 1 mL EtOH, 1 mL heteroarene, 2 mg 3D Fe₃O₄@Cu_{2-x}S-MoS₂F, irradiation with Xenon lamp equipped with 700nm cutoff filter for 1 h under argon atmosphere. All the yields were determined by GC.

Good recyclability is the main superiority of heterogeneous catalysts. The reusability of Fe₃O₄@Cu_{2-x}S-MoS₂F catalyst in the direct arylation of heteroarenes between aryldiazonium tetrafluoroborate with furan was also tested. The active material was separated from the reaction mixture via magnet, and reused directly for 6 times. To our delight, no obvious deactivation was observed. The yield of the desired product amounted to 93% at the sixth cycle (Figure 4A). Meanwhile, the TEM and SEM results of the used catalyst show no obvious change in morphology or aggregation of the Fe₃O₄@Cu_{2-x}S-MoS₂F and Fe₃O₄@Cu_{2-x}S nanoparticles (Figure S14), showing a good recyclability in this type of photocatalytic arylation of heteroarenes reactions.

A plausible mechanism for this photoreaction is depicted in Figure 4B, similar to used TiO₂ catalyst.²⁵ Based on our findings (Figure S15 as well as related discussions in the

supporting information) and some literature reports, we concluded that the diazonium salt reacts with the ethanol to form the azoether 4,²⁵ and then the aryl radical 5 is produced by a single-electron transfer (SET) from the excited state of photocatalyst $\text{Fe}_3\text{O}_4@\text{Cu}_{2-x}\text{S}-\text{MoS}_2\text{F}$. Addition of aryl radical 5 to heteroaromatic 2 forms radical intermediate 6, which is further oxidized by photocatalyst or by azoether 4 in a radical chain transfer mechanism to give carbocation intermediate 7. The desired coupling product 3 was formed by the rearomatization of 7. In addition, the more efficient adsorption of substrate molecules on MoS_2 provides a high concentration of substrates near to the $\text{Fe}_3\text{O}_4@\text{Cu}_{2-x}\text{S}$ NPs inserted between the layers of MoS_2 , leading to highly efficient contact between them. Thus the photocatalytic process is promoted.

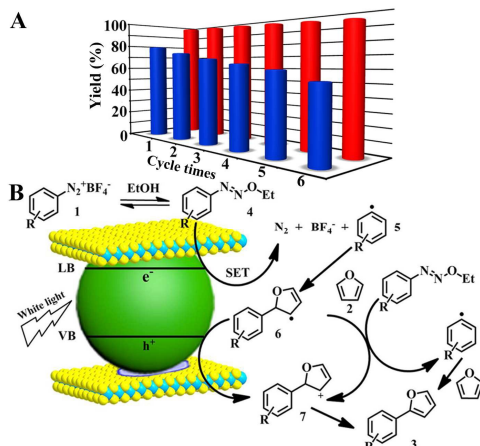


Figure 4. (A) Catalytic cycle of the $\text{Fe}_3\text{O}_4@\text{Cu}_{2-x}\text{S}$ nanoparticles (blue column) and the 3D $\text{Fe}_3\text{O}_4@\text{Cu}_{2-x}\text{S}-\text{MoS}_2\text{F}$ (red column). (B) Postulated reaction mechanism for the 3D $\text{Fe}_3\text{O}_4@\text{Cu}_{2-x}\text{S}-\text{MoS}_2\text{F}$ -mediated direct arylation of heteroarenes.

In summary, a new porous MoS_2 -based framework was successfully synthesized by covalent functionalization of exfoliated MoS_2 nanosheets with LA-DPA followed by coordination with $\text{Fe}_3\text{O}_4@\text{Cu}_{2-x}\text{S}$ NPs. The novel, MoS_2 -based catalyst exhibits excellent NIR- light-driven photocatalytic activity and stable cycling for the direct arylation of heteroarenes at room temperature, superior to those of MoS_2 , $\text{Fe}_3\text{O}_4@\text{Cu}_{2-x}\text{S}$, simply mixed $\text{Fe}_3\text{O}_4@\text{Cu}_{2-x}\text{S}$ and MoS_2 samples, and recently reported photocatalysts. The improved photocatalytic activity of such hybrid framework may be associated with abundant porosity, high specific surface area, the enhanced adsorption capacity to substrates, good NIR light capture, and good structural stability. Thus, such 3D MoS_2 based-frameworks show the potential to use solar energy. Our findings pave the way to build reliable 3D MoS_2 hybrid frameworks for the expanding utilization of solar light and achieving high photocatalytic efficiency.

Notes and references

^aKey Laboratory of Nonferrous Metal Chemistry and Resources Utilization of Gansu Province and State Key Laboratory of Applied Organic Chemistry Lanzhou University Gansu, Lanzhou, 730000 (P.R. China) Lanzhou University, China. E-mail: wangbd@lzu.edu.cn.

†Electronic Supplementary Information (ESI) available: [Experimental details, synthesis and characterization]. See DOI: 10.1039/b000000x/

‡This work was supported by the National Natural Science Foundation of China (21271093, 21431002, and 21401091), the National Basic Research Program of China (973 Program, 2012CB932500), the NCET

(13-0262), and the Fundamental Research Funds for the Central Universities (lzujbky-2014-k06).

- (a) D. Gust, T. A. Moore and A. L. Moore, *Acc. Chem. Res.*, 2009, **42**, 1890-1898. (b) J. Barber, *Chem. Soc. Rev.*, 2009, **38**, 185-196.
- S. Cho, M. J. Lee, M. S. Kim, S. Lee, Y. K. Kim, D. H. Lee, C. W. Lee, H. Cho and J. H. Chung, *J. Dermatol. Sci.*, 2008, **50**, 123-133.
- (a) J. B. Cui, Y. J. Li, L. Liu, L. Chen, J. Xu, J. W. Ma, G. Fang, E. Zhu, H. Wu, L. X. Zhao, L. Y. Wang and Y. Huang, *Nano Lett.*, 2015, **15**, 6295-6301. (b) Y. N. Tang, W. H. Di, X. S. Zhai, R. Y. Yang and W. P. Qin, *ACS Catal.*, 2013, **3**, 405-412. (c) G. W. Cui, W. Wang, M. Y. Ma, J. F. Xie, X. F. Shi, N. Deng, J. P. Xin and B. Tang, *Nano Lett.*, 2015, **15**, 7199-7203.
- (a) B. Radisavljevic, A. Radenovic, J. Brivio, V. Giacometti and A. Kis, *Nat. Nanotechnol.*, 2011, **6**, 147-150. (b) Q. H. Wang, K. Kalantar-Zadeh, A. Kis, J. N. Coleman and M. S. Strano, *Nat. Nanotechnol.*, 2012, **7**, 699-712.
- (a) A. Splendiani, L. Sun, Y. Zhang, T. Li, J. Kim, C.-Y. Chim, G. Galli and F. Wang, *Nano Lett.*, 2010, **10**, 1271-1275. (b) K. F. Mak, C. Lee, J. Hone, J. Shan and T. F. Heinz, *Phys. Rev. Lett.*, 2010, **105**, 136805. (c) K. F. Mak, K. He, J. Shan and T. F. Heinz, *Nat. Nanotechnol.*, 2012, **7**, 494-498.
- (a) B. Hinnemann, P. G. Moses, J. Bonde, K. P. Jørgensen, J. H. Nielsen, S. Hørch, I. Chorkendorff and J. K. Nørskov, *J. Am. Chem. Soc.*, 2005, **127**, 5308-5309. (b) M. Chhowalla, H. S. Shin, G. Eda, L. J. Li, K. P. Loh and H. Zhang, *Nat. Chem.*, 2013, **5**, 263-275. (c) Y. Yu, S.-Y. Huang, Y. Li, S. N. Steinmann, W. Yang and L. Cao, *Nano Lett.*, 2014, **14**, 553-558. (d) J. P. Wilcoxon, *J. Phys. Chem. B*, 2000, **104**, 7334-7343.
- W. K. Ho, J. C. Yu, J. Lin, J. G. Yu and P. S. Li, *Langmuir*, 2004, **20**, 5865-5869.
- (a) L. Zhang, H. B. Wu, Y. Yan, X. Wang and X. W. Lou, *Energy Environ. Sci.*, 2014, **7**, 3302-3306. (b) P. P. Wang, H. Y. Sun, Y. J. Ji, W. H. Li and X. Wang, *Adv. Mater.*, 2014, **26**, 964-969.
- (a) I. Bezhverkhy, P. Afanasiev and M. Lacroix, *Inorg. Chem.*, 2000, **39**, 5416-5417. (b) G. Alonso, G. Berhault, F. Paraguay, E. Rivera, S. Fuentes and R. Chianelli, *Mater. Res. Bull.*, 2003, **38**, 1045-1055. (c) G. Alonso, M. Valle, J. Cruz, V. Petranovskii, A. Licea-Claverie and S. Fuentes, *Catal. Today*, 1998, **43**, 117-122. (d) W. Li, E. Shi, J. Ko, Z. Chen, H. Ogino and T. J. Fukuda, *Cryst. Growth*, 2003, **250**, 418-422.
- Q. W. Tian, J. Q. Hu, Y. H. Zhu, R. J. Zou, Z. G. Chen, S. P. Yang, R. W. Li, Q. Q. Su, Y. Han and X. G. Liu, *J. Am. Chem. Soc.*, 2013, **135**, 8571-8577.
- S. S. Chou, M. De, J. Kim, S. Byun, C. Dykstra, J. Yu, J. X. Huang and V. P. Dravid, *J. Am. Chem. Soc.*, 2013, **135**, 4584-4587.
- (a) W. J. Zhou, K. Zhou, D. Hou, X. J. Liu, G. Q. Li, Y. H. Sang, H. Liu, L. G. Li and S. W. Chen, *ACS Appl. Mater. Interfaces*, 2014, **6**, 21534-21540. (b) J. Xie, J. Zhang, S. Li, F. Grote, X. Zhang, H. Zhang, R. Wang, Y. Lei, B. Pan and Y. Xie, *J. Am. Chem. Soc.*, 2013, **135**, 17881-17888. (c) Y. G. Li, H. L. Wang, L. M. Xie, Y. Y. Liang, G. S. Hong and H. J. Dai, *J. Am. Chem. Soc.*, 2011, **133**, 7296-7299. (d) Z. Y. Sui, Y. N. Meng, P. W. Xiao, Z. Q. Zhao, Z. X. Wei and B. H. Han, *ACS Appl. Mater. Interfaces*, 2015, **7**, 1431-1438.
- (a) S. Stankovich, D. A. Dikin, R. D. Piner, K. A. Kohlhaas, A. Kleinhammes, Y. Jia, Y. Wu, S. T. Nguyen, R. S. Ruoff, *Carbon* 2007, **45**, 1558-1565. (b) J.H. Lee, N.Park, B. G. Kim, D. S. Jung, K. Im, J. Hur, J. W. Choi, *ACS NANO*, 2013, **7**, 9366-9374.
- (a) Y. Zhao, H. Pan, Y. Lou, X. Qiu, J. Zhu and C. Burda, *J. Am. Chem. Soc.*, 2009, **131**, 4253-4261. (b) J. M. Luther, P. K. Jain, T. Ewers and A. P. Alivisatos, *Nat. Mater.*, 2011, **10**, 361-366.
- H. Wang, K. Sun, F. Tao, D. J. Stacchiola and Y. H. Hu, *Angew. Chem., Int. Ed.*, 2013, **52**, 9210-9214.
- L. L. Li, X. B. Chen, Y. E. Wu, D. S. Wang, Q. Peng, G. Zhou and Y. D. Li, *Angew. Chem., Int. Ed.*, 2013, **52**, 11049-11053.
- (a) A. R. Murphy and J. M. J. Fréchet, *Chem. Rev.*, 2007, **107**, 1066-1096. (b) J. E. Anthony, *Chem. Rev.*, 2006, **106**, 5028-5048. (c) J. Mei, K. R. Graham, R. Stalder and J. R. Reynolds, *Org. Lett.*, 2010, **12**, 660-663. (d) H. Dong, C. Wang and W. Hu, *Chem. Commun.*, 2010, **46**, 5211-5222.
- (a) H. Yin, G.-i. Lee, H. S. Park, G. A. Payne, J. M. Rodriguez, S. M. Sebt and A. D. Hamilton, *Angew. Chem., Int. Ed.*, 2005, **44**, 2764-2767. (b) O. Kutzki, H. S. Park, J. T. Ernst, B. P. Orner, H. Yin and A. D. Hamilton, *J. Am. Chem. Soc.*, 2002, **124**, 11838-11839.
- (a) J. O. Trent, G. R. Clark, A. Kumar, W. D. Wilson, D. W. Boykin, J. E. Hall, R. R. Tidwell, B. L. Blagburn and S. Neidle, *J. Med. Chem.*, 1996, **39**, 4554-4562. (b) B. Schmidt and D. Geißler, *Eur. J. Org. Chem.*, 2011, 4814-4822. (c) Y. I. Gorak, N. D. Obushak, V. S. Matiichuk and R. Z. Lytvyn, *Russ. J. Org. Chem.*, 2009, **45**, 541-550.
- (a) K. Zeitler, *Angew. Chem., Int. Ed.*, 2009, **48**, 9785-9789. (b) T. P. Yoon, M. A. Ischay and J. Du, *Nat. Chem.*, 2010, **2**, 527-532. (c) J. Xuan and W. Xiao, *Angew. Chem., Int. Ed.*, 2012, **51**, 6828-6838.
- (a) D. P. Hari, P. Schroll and B. König, *J. Am. Chem. Soc.*, 2012, **134**, 2958-2961. (b) C. Galli, *Chem. Rev.*, 1988, **88**, 765-792.
- J. Zoller, D. C. Fabry and M. Rueping, *ACS Catal.*, 2015, **5**, 3900-3904.